Monosynaptic Projections to Excitatory and Inhibitory preBötzinger Complex Neurons

Cindy F. Yang[1], Euiseok J. Kim[2†], Edward M. Callaway[2] and Jack L. Feldman[1*]

[1] Department of Neurobiology, David Geffen School of Medicine, University of California, Los Angeles, Los Angeles, CA, United States, [2] Systems Neurobiology Laboratory, Salk Institute for Biological Studies, La Jolla, CA, United States

The key driver of breathing rhythm is the preBötzinger Complex (preBötC) whose activity is modulated by various functional inputs, e.g., volitional, physiological, and emotional. While the preBötC is highly interconnected with other regions of the breathing central pattern generator (bCPG) in the brainstem, there is no data about the direct projections to either excitatory and inhibitory preBötC subpopulations from other elements of the bCPG or from suprapontine regions. Using modified rabies tracing, we identified neurons throughout the brain that send monosynaptic projections to identified excitatory and inhibitory preBötC neurons in mice. Within the brainstem, neurons from sites in the bCPG, including the contralateral preBötC, Bötzinger Complex, the nucleus of the solitary tract (NTS), parafacial region (pF_L/pF_V), and parabrachial nuclei (PB), send direct projections to both excitatory and inhibitory preBötC neurons. Suprapontine inputs to the excitatory and inhibitory preBötC neurons include the superior colliculus, red nucleus, amygdala, hypothalamus, and cortex; these projections represent potential direct pathways for volitional, emotional, and physiological control of breathing.

Keywords: breathing, neural circuit, respiration, modified rabies, retrograde tracing, afferent tracing, preBötzinger Complex

INTRODUCTION

Breathing is a remarkable behavior that sustains a robust and precisely modulated rhythmic movement appropriate across all behaviors and states, including for: (i) homeostatic regulation of blood gas and pH levels, (ii) volitional control of airflow for speech, breath-holding, etc., (iii) emotional control of airflow for laughing, crying, sighing, etc., and (iv) sleep and wakefulness. Moreover, breathing is highly sensitive to changes in stress; high levels of stress are associated with hyperventilation, while low levels of stress are associated with slow deep breathing (Boiten et al., 1994). The kernel of the breathing central pattern generator (bCPG) resides in the preBötzinger Complex (preBötC), a small cluster of neurons in the ventrolateral medulla that underlies breathing rhythmogenesis to ultimately drive periodic inspiratory movements (Del Negro et al., 2018). How the brain modulates breathing by actions within the preBötC across different behaviors and states is largely unknown.

Likely substrates for such modulation are subpopulations of preBötC neurons that receive signals from regulatory brain centers such as the hypothalamus, which monitors and controls many important aspects of physiological state, e.g., temperature, arousal, and pregnancy, the limbic system related to emotional control of breathing, and cortical structures that control volitional movements that involve breathing, e.g., speech, breath-holding. The regions of the brain that project to and innervate the preBötC have been broadly identified. Indeed, brain regions such as the lateral and paraventricular hypothalamus, the central amygdala, orbital cortex, and various raphe and brainstem nuclei, are sources of afferent projections to the bCPG (Gang et al., 1995). However, retrograde tracers used in these studies were not specific to neuronal subtypes, e.g., excitatory vs. inhibitory neurons, and could have been taken up by fibers of passage that could underlie false positives, motivating the present study.

Since molecular diversity across neuronal subpopulations can be a substrate for differences in afferent projections contributing to functional heterogeneity, specificity is critical when mapping a neural circuit. Particularly, the preBötC is comprised of a mix of excitatory (glutamatergic) and inhibitory (glycinergic and GABAergic) neurons that can be further segregated based on gene expression, e.g., glutamatergic excitatory preBötC neurons can express neurokinin 1 and/or μ-opioid receptors, the peptide somatostatin (SST), the transcription factor Dbx1 (transiently), and/or Reelin (Feldman et al., 2013). Of these molecular subtypes, we focused on preBötC SST-expressing neurons, which are glutamatergic, and neurons that express the glycine transporter GlyT2, which comprise a fraction of the preBötC excitatory and inhibitory subpopulation (∼17 and ∼50%), respectively (Stornetta et al., 2003; Morgado-Valle et al., 2010; Sherman et al., 2015; Cui et al., 2016). While SST- and GlyT2-expressing neurons are not required for rhythmogenesis, they play a critical role in transmitting signals related to inspiratory movements to preBötC targets and can modulate respiratory pattern and drive apneas, respectively (Tan et al., 2008; Sherman et al., 2015; Cui et al., 2016). Determining the specific projections onto each of these subpopulations of excitatory and inhibitory neurons is critical to ultimately understanding how breathing is modulated by behavior and state.

We examined projections to excitatory SST$^+$ or inhibitory GlyT2$^+$ preBötC neurons by targeting modified rabies virus (EnvA + RVdG-mCherry) to the preBötC of Cre-expressing mice. This allows retrograde tracing restricted to one synapse, revealing neurons with direct, i.e., monosynaptic, inputs to preBötC. We found that within the brainstem, preBötC neurons receive inputs from other brainstem bCPG regions including contralateral preBötC, Bötzinger Complex, intermediate reticular region, the nucleus of the solitary tract (NTS), and parabrachial nuclei/Kölliker-Fuse (PB/KF). Suprapontine regions that provide direct input to the preBötC include the periaqueductal gray (PAG), superior colliculus, substantia nigra, central amygdala (CeA), and cortex. Interestingly, neither brainstem nor suprapontine projections discriminated between excitatory or inhibitory targets, as excitatory SST$^+$ and inhibitory GlyT2$^+$ preBötC neurons both received projections from the same regions, suggesting that the magnitude and even sign

of modulation of breathing related to emotional, cognitive, physiological, and behavioral functions may be determined by the balance of inputs to these subpopulations.

MATERIALS AND METHODS

Animals

Animal use was in accordance with the guidelines approved by the UCLA Institutional Animal Care and Use Committee. Animals were housed in a vivarium under a 12 h light cycle with free access to food and water. All experiments were performed using adult male SST-Cre and GlyT2-Cre mice (24–30 g) that were 10–24 weeks of age at the time of AAV injection. SST-Cre (IMSR Cat# JAX:013044, RRID: IMSR_JAX:013044) mice were crossed to Cre-reporter mice (IMSR Cat# JAX:004077, RRID: IMSR_JAX:004077) to generate the SST reporter line used in the tracing studies. Prior to surgery, animals were group housed in cages of up to 5 mice, and after surgery, animals were individually housed. GlyT2-Cre mice were kindly provided by H. U. Zeilhofer, University of Zurich, Switzerland (Foster et al., 2015), and all other mice were obtained from Jackson Labs (Bar Harbor, ME, United States).

Viruses

For rabies virus tracing, two Cre-dependent helper viruses, AAV8-EF1α-FLEX-BFP-T2A-TVA-WPRE-hGH (3.5 × 10^{13} GC/ml) (EK/EC unpublished) (referred to in the text as AAV-FLEX-BFP-TVA) and AAV8-EF1α-FLEX-G -WPRE-hGH (7.6 × 10^{13} GC/ml) expressing chimeric rabies glycoprotein (PBG) (AAV-FLEX-G), were produced by the Salk Viral Vector Core. PBG is a chimeric glycoprotein consisting cytoplasmic domain of SAD B19 strain glycoprotein and extracellular domain of Pasteur virus strain glycoprotein (Kim et al., 2016). A 3:7 mixture of AAV-FLEX-BFP-TVA and AAV-FLEX-G was used for viral injections. EnvA-pseudotyped G-deleted rabies virus, EnvA + RVdG-mCherry, with the titer of 3.6 × 10^7 infectious units (IU/ml), was provided by the Salk Viral Vector Core.

Surgical Procedures

All experimental procedures were approved by the Chancellor's Animal Research Committee at the University of California, Los Angeles, and modified rabies experiments were performed according to the biosafety guidelines of the UCLA Office of Environment, Health, and Safety. For AAV iontophoresis injections, male mice (10–24 weeks old) were anesthetized with isoflurane and positioned in a stereotaxic apparatus (Kopf Instruments, Tujunga, CA, United States). The skull was exposed with a midline scalp incision, and the stereotaxic frame was aligned at bregma using visual landmarks. A drill was placed over the skull at the coordinates corresponding to the preBötC (anteroposterior, -6.78 mm; lateral, 1.25 mm) (Paxinos and Franklin, 2004), and a hole was drilled through the skull bone to expose the cerebellum. A micropipette (∼20 μm tip I.D.) loaded with virus (AAV-FLEX-BFP-TVA and AAV-FLEX-G) was aligned at bregma (including in the z-axis), guided to

the preBötC coordinates, and slowly lowered at 1 mm/min until it penetrated to a depth of -4.8 mm. A silver wire electrode was inserted into the micropipette, with the tip submerged in the viral solution, and was connected to a current source (Midgard Electronics, Watertown, MA, United States). A current of 3 μA (7 s on, 7 s off) was applied for 5 min, and the micropipette was left in place for 10 min to allow viral particles to diffuse and then withdrawn at 1 mm/min to minimize the backflow along the micropipette track. After surgery, mice were housed for 3 weeks to allow robust expression. For injection of the modified rabies virus, a second surgery was performed as above, but a Picospritzer pressure injection system was used to dispense 20–40 nl of EnvA + RV*dG*-mCherry rabies (Salk Institute Viral Vector Core). After 7–10 days we processed the brains for histology, using anatomical landmarks, e.g., facial and hypoglossal nuclei, and nucleus ambiguus, to verify that the starter cells were localized to the preBötC.

To identify the molecular phenotype of retrogradely labeled preBötC neurons, iontophoresis of Fluorogold in to the preBötC was performed as described above for AAV injections using a micropipette (∼30 μm tip I.D.) containing 1% Fluorogold solution with an application of 5 μA of current for 7 min (7 s on, 7 s off). After surgery, mice were housed for 8–10 days before their brains were processed for histology.

Histology

Mice transfected with AAV and modified rabies viruses were processed as previously described (Sherman et al., 2015; Yang and Feldman, 2018). Briefly, mice were deeply anesthetized with isoflurane and perfused transcardially with saline followed by 4% paraformaldehyde in phosphate-buffered saline (PBS). Brains were removed, postfixed overnight at 4°C, and embedded in 3% Bacto agar. Free-floating coronal or sagittal sections (40 μm) were collected using a vibratome (Leica Biosystems, Buffalo Grove, IL, United States) and stored at 4°C until further processing. Sections were incubated with primary antibodies in PBS containing 0.3% Triton X-100 overnight at room temperature. After three washes, sections were incubated in species-appropriate secondary antibodies in PBS for 2 h at room temperature. After three washes, sections were mounted onto gelatin-treated glass slides and coverslipped. Fluorescence was visualized with a confocal laser scanning microscope (LSM710; Carl Zeiss, Oberkochen, Germany). Images were acquired with Zen software (Carl Zeiss), exported as TIFF files, processed in Image J (NIH, Bethesda, MD, United States; RRID: SCR_003070NIH), and assembled in Adobe Illustrator. The preBötC was localized using anatomical landmarks and based on the following criteria: ∼500 μm posterior to the facial nucleus, immediately dorsal to the nucleus ambiguus (extending from the semi-compact to the loose subnuclei), with a hatched appearance by brightfield microscopy and diameter of ∼500 μm. Facial nucleus and nucleus ambiguus could be visualized by choline acetyltransferase (ChAT) staining, and the preBötC by a concentration of SST-expressing neurons. For immunostaining, goat polyclonal anti-choline acetyltransferase (AB144P, 1:500,
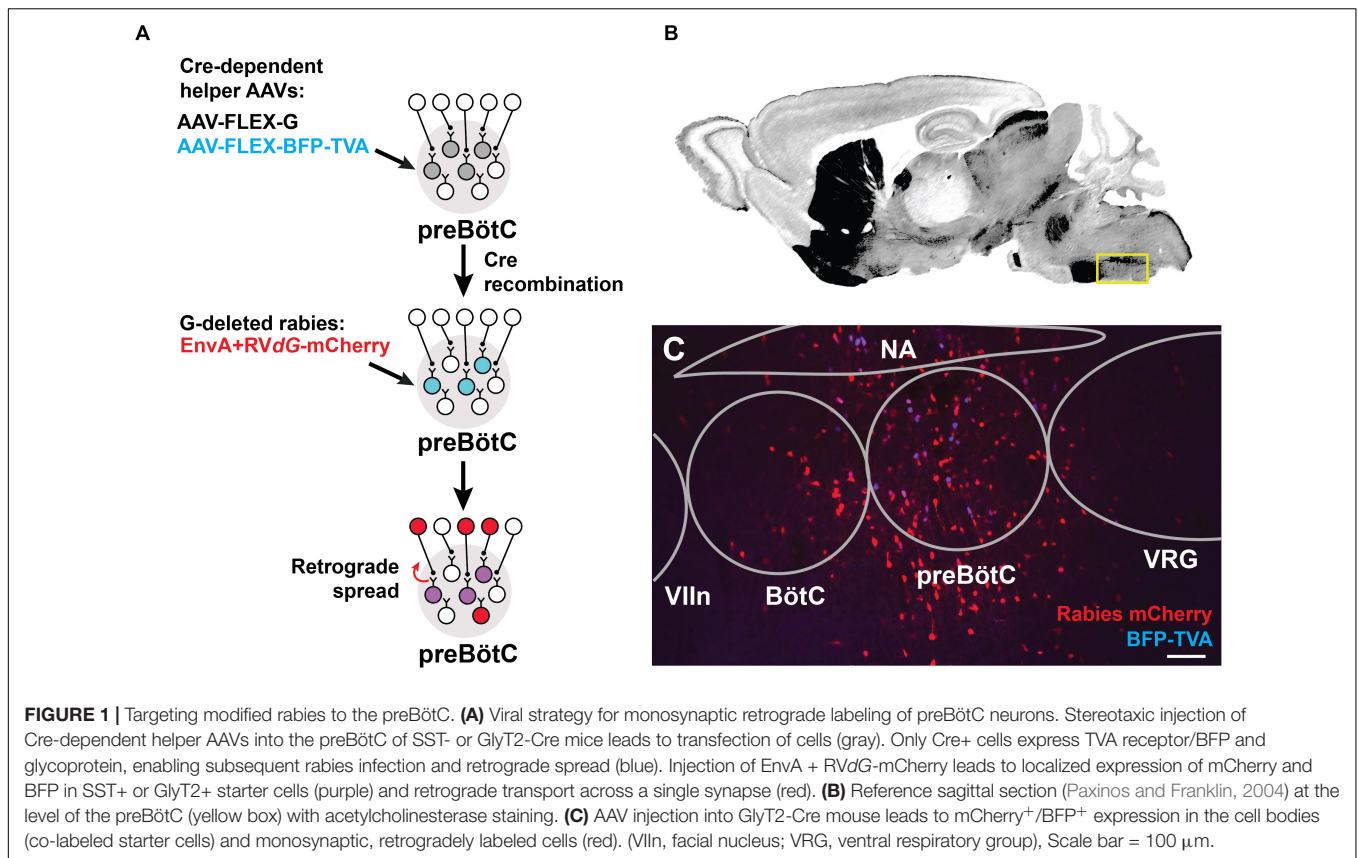
Millipore, RRID: AB_2079751) and donkey anti-goat rhodamine Red-X conjugated antibodies (1:250; Jackson ImmunoResearch, West Grove, PA, United States) were used.

RESULTS

Targeting SST[+] and GlyT2^{+} preBötC Neurons

We identified sources of direct afferent input to subpopulations of preBötC neurons using transsynaptic retrograde labeling with modified rabies virus (Wickersham et al., 2013; Kim et al., 2016). This genetic strategy requires two stages (**Figure 1A**): (i) Introduction of Cre-dependent helper viruses into the preBötC of SST-Cre or GlyT2-Cre mice for genetic specificity. The helper viruses, AAV-FLEX-BFP-TVA and AAV-FLEX-G, encode for the avian sarcoma leucosis virus glycoprotein receptor, TVA (not normally expressed in mammals), and for an optimized rabies glycoprotein required for retrograde transport, respectively. (ii) Subsequent delivery of an EnvA-pseudotyped rabies virus for retrograde tracing. Since the rabies virus cannot infect cells in the absence of the TVA receptor, infection is limited to Cre^{+} cells expressing the helper AAV. This modified rabies virus bears a deletion of the endogenous glycoprotein G that is replaced with the coding sequence for mCherry (EnvA + RV*dG*-mCherry), rendering it incapable of retrograde transport. Thus, only in Cre^{+} cells complemented with the glycoprotein via helper AAV injection will the rabies virus be able to cross the synapse to label presynaptic neurons. Presynaptic neurons do not express the glycoprotein, thus restricting viral transfer and ensuring monosynaptic retrograde spread.

Cells infected by the rabies virus express mCherry, and co-expression of BFP from the helper AAVs enabled the identification of the putative initial Cre[+] starter population at the preBötC, which was localized based on relative distance to anatomical landmarks, e.g., facial nucleus and nucleus ambiguus (see Methods, **Figures 1B,C**). Neurons immediately presynaptic to the preBötC were identified as singly positive for mCherry. We note that the rabies virus may have expressed in non-Cre^{+} neurons, possibly due to the leak expression of the TVA receptor, but these neurons would not be capable of long-distance, *trans*-synaptic rabies transfer without coincident leak expression of the glycoprotein (Wall et al., 2010; Miyamichi et al., 2013; Kim et al., 2015). Furthermore, we did not observe TVA receptor/BFP expression more than 1 mm beyond the injection site, but we do not discount the presence of lower levels of expression that we could not detect. Injection of the rabies virus alone without the helper viruses labeled 2–3 cells at the injection site (n = 2), but not beyond. Data was discarded from experiments where there was mistargeting or extensive mCherry[+]/BFP^{+} neurons along the micropipette track or neighboring regions. We analyzed data from experiments in which mCherry[+]/BFP^{+} neurons were mostly restricted to the preBötC (86 ± 15 cells SST-Cre; 65 ± 20 cells GlyT2-Cre), with minimal double-labeled starter cells found in neighboring regions (11 ± 8 cells SST-Cre; 13 ± 4 cells GlyT2-Cre; **Figure 1C**). Here we report the sources of afferent projections to SST[+] and GlyT2^{+} preBötC neurons

FIGURE 1 | Targeting modified rabies to the preBötC. **(A)** Viral strategy for monosynaptic retrograde labeling of preBötC neurons. Stereotaxic injection of Cre-dependent helper AAVs into the preBötC of SST- or GlyT2-Cre mice leads to transfection of cells (gray). Only Cre+ cells express TVA receptor/BFP and glycoprotein, enabling subsequent rabies infection and retrograde spread (blue). Injection of EnvA + RV*dG*-mCherry leads to localized expression of mCherry and BFP in SST+ or GlyT2+ starter cells (purple) and retrograde transport across a single synapse (red). **(B)** Reference sagittal section (Paxinos and Franklin, 2004) at the level of the preBötC (yellow box) with acetylcholinesterase staining. **(C)** AAV injection into GlyT2-Cre mouse leads to mCherry⁺/BFP⁺ expression in the cell bodies (co-labeled starter cells) and monosynaptic, retrogradely labeled cells (red). (VIIn, facial nucleus; VRG, ventral respiratory group), Scale bar = 100 µm.

that were observed across multiple experiments ($n = 5$ SST-Cre, $n = 4$ GlyT2-Cre).

Given the small size of the preBötC (∼500 µm across) and the inherent sparse labeling of the modified rabies strategy (Callaway and Luo, 2015), we anticipated the possibility of false negatives, i.e., inability to detect some afferent projections. To get a handle on false negatives, we first used a non-genetic approach to compile a more comprehensive list of brain regions projecting to the preBötC (and its immediate surround). We injected Fluorogold unilaterally to the preBötC ($n = 4$; **Supplementary Figure S1A**) and found retrograde labeling in many brainstem and suprapontine sites, including BötC, facial (VIIn) and hypoglossal (XIIn) nuclei, NTS, parahypoglossal region, PB/KF, the red nucleus, substantia nigra, motor and sensory cortex, as well as the hypothalamus and amygdala (**Supplementary Figures S1B–P**). With this general map of afferent projections to the vicinity of the preBötC, we then carefully scrutinized these regions for neurons infected using the modified rabies strategy.
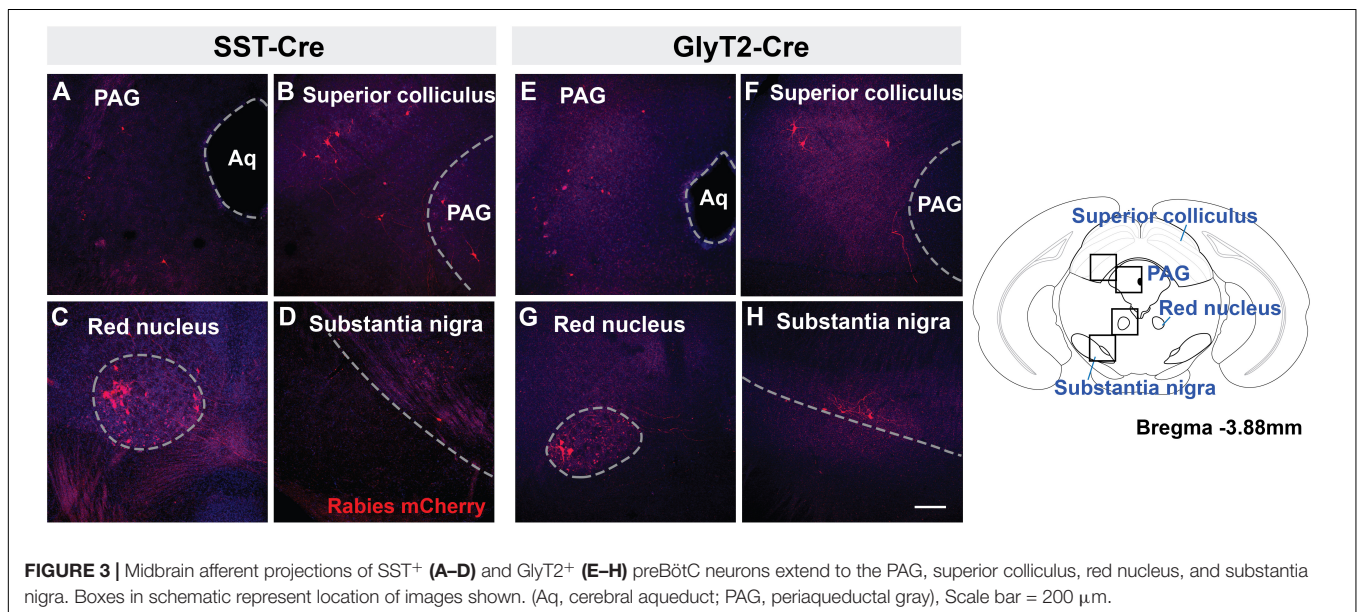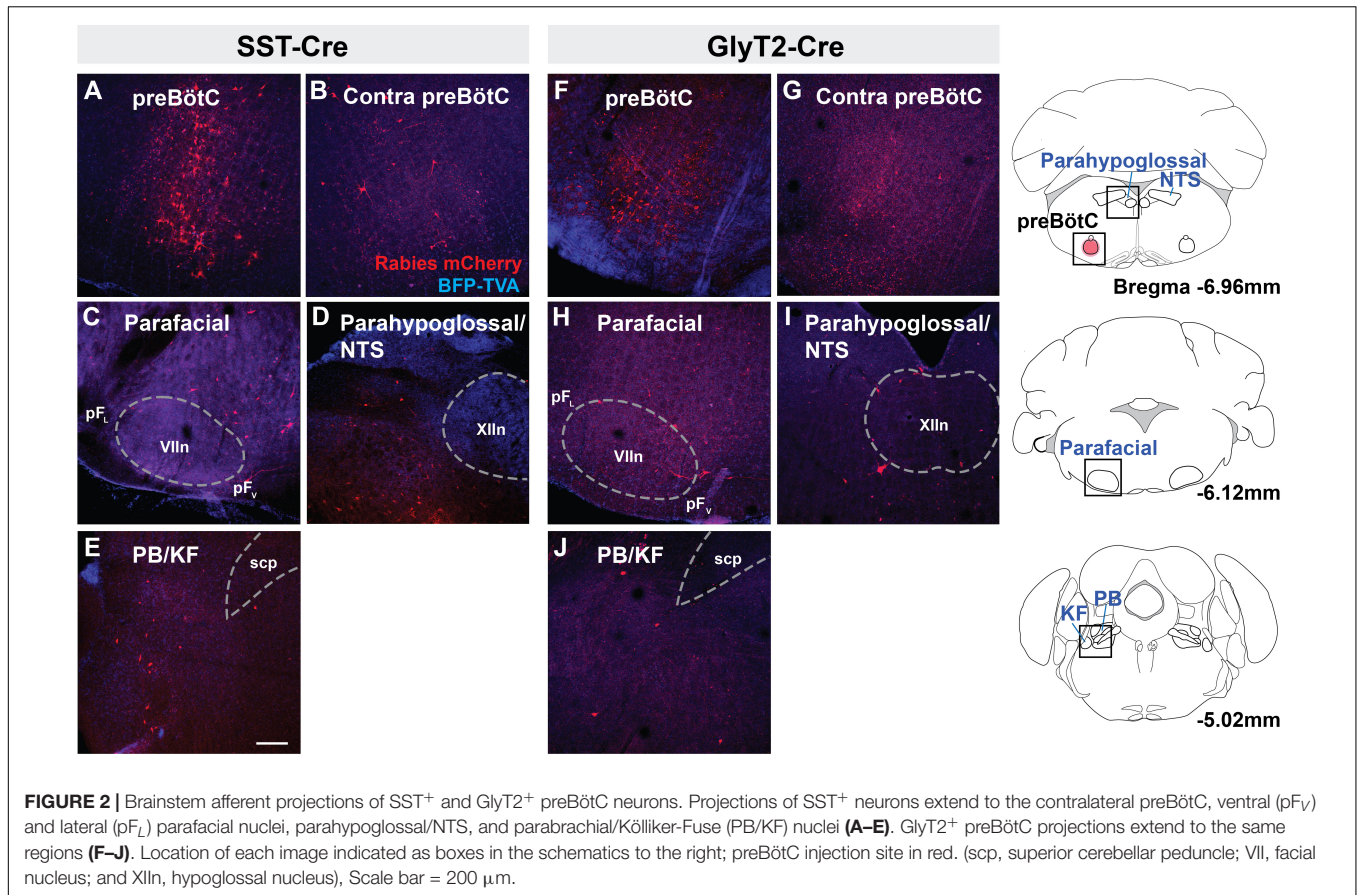
Afferent Projections From Brainstem to preBötC Neurons

Rabies virus injected SST-Cre mouse brains had scattered mCherry⁺ neurons in the preBötC and surround, indicating that virally infected preBötC neurons also receive synaptic input from local preBötC neurons (**Figures 2A,B**). This spread of mCherry⁺ cells extended rostrally through the Bötzinger Complex with

some neurons found in the parafacial ventral nucleus (pF$_V$) and few in the lateral nucleus (pF$_L$) (**Figure 2C**) (Huckstepp et al., 2016). Among dorsal regions, mCherry⁺ neurons were found in the NTS and parahypoglossal region and throughout the intermediate reticular nucleus (**Figure 2D** and not shown). Some of these labeled neurons were dorsomedial to the BötC, corresponding to the region dubbed the "pre-inspiratory complex" (PiCo) (Anderson et al., 2016) (not shown). Within the pons, mCherry⁺ neurons were found in the dorsolateral, medial parabrachial nucleus, KF, and around the trigeminal nucleus (**Figure 2E**, not shown). There were occasional neurons in the pontine reticular nuclei. In rabies-injected GlyT2-Cre mouse brains, mCherry⁺ neurons were found in all of the same regions as identified in SST-Cre injected mice though with qualitatively sparser labeling (**Figures 2F–J**). In both SST- and GlyT2-Cre mice, mCherry⁺ neurons were visible bilaterally in any given structure, but more neurons were present on the side ipsilateral to the injection. Thus, we found that afferent projections from the same brainstem sites can innervate both excitatory SST⁺ and inhibitory GlyT2⁺ preBötC neurons.

Suprapontine Projections to preBötC Neurons

Retrogradely labeled neurons were found in all of the same midbrain regions in both SST-Cre and GlyT2-Cre mice (**Figure 3**). mCherry⁺ neurons were located bilaterally, though more neurons were found on the side contralateral to the

FIGURE 2 | Brainstem afferent projections of SST$^+$ and GlyT2$^+$ preBötC neurons. Projections of SST$^+$ neurons extend to the contralateral preBötC, ventral (pF$_V$) and lateral (pF$_L$) parafacial nuclei, parahypoglossal/NTS, and parabrachial/Kölliker-Fuse (PB/KF) nuclei **(A–E)**. GlyT2$^+$ preBötC projections extend to the same regions **(F–J)**. Location of each image indicated as boxes in the schematics to the right; preBötC injection site in red. (scp, superior cerebellar peduncle; VII, facial nucleus; and XIIn, hypoglossal nucleus), Scale bar = 200 μm.

FIGURE 3 | Midbrain afferent projections of SST$^+$ **(A–D)** and GlyT2$^+$ **(E–H)** preBötC neurons extend to the PAG, superior colliculus, red nucleus, and substantia nigra. Boxes in schematic represent location of images shown. (Aq, cerebral aqueduct; PAG, periaqueductal gray), Scale bar = 200 μm.

injection. Labeled neurons were observed in the in the dorsolateral PAG (**Figures 3A,E**) as well as the superior, but not in the inferior, colliculus (**Figures 3B,F**). In some instances (n = 3 of 5 SST-Cre and n = 3 of 4 GlyT2-Cre), neurons in the lateral portion of the magnocellular red nucleus were also labeled (**Figures 3C,G**). On rare occasion (n = 2 of 5 SST-Cre and n = 1 of 4 GlyT2-Cre), mCherry-labeled neurons were found in the dorsal raphe nucleus and in or bordering the substantia nigra pars compacta (**Figures 3D,H**).
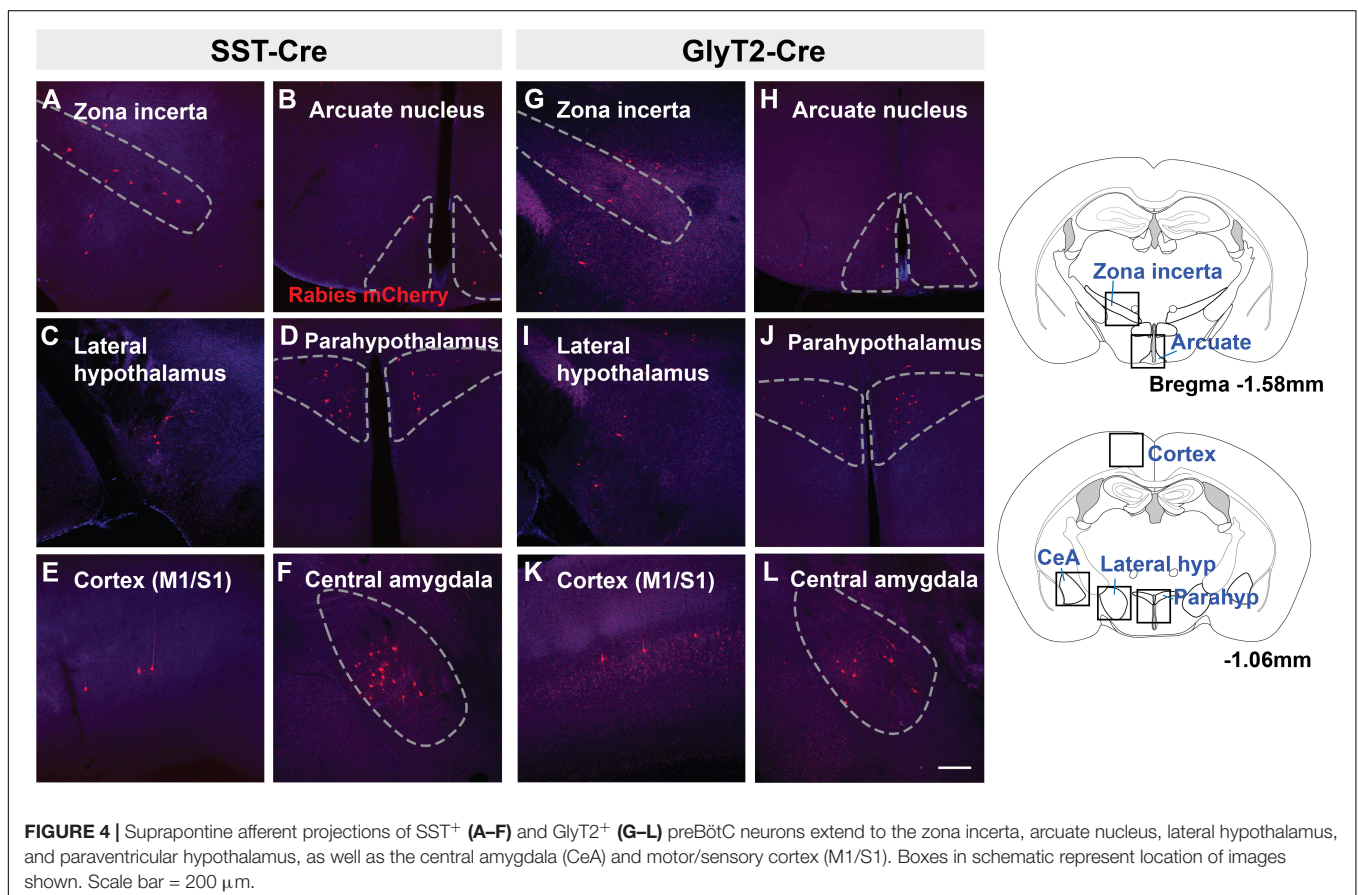
There were fewer mCherry-labeled neurons rostral to the midbrain, with <20 neurons in each identified region. We found mCherry$^+$ neurons in the zona incerta (**Figures 4A,G**) and various compartments of the hypothalamus, including the arcuate nucleus (**Figures 4B,H**) lateral and dorsomedial hypothalamic nuclei (**Figures 4C,I**), and medial preoptic area. For each of the SST-Cre and GlyT2-Cre cohorts, a few retrogradely labeled neurons were found in the ventromedial and paraventricular hypothalamic nuclei (n = 2 of 5 SST-Cre and 2 of 4 GlyT2-Cre, **Figures 4D,J**), the bed nucleus of the stria terminalis (n = 2 of 5 SST-Cre and 1 of 4 GlyT2-Cre), the anteroventral periventricular nucleus of the hypothalamus, and the basal forebrain (n = 1 of 5 SST-Cre and 1 of 4 GlyT2-Cre, data not shown).
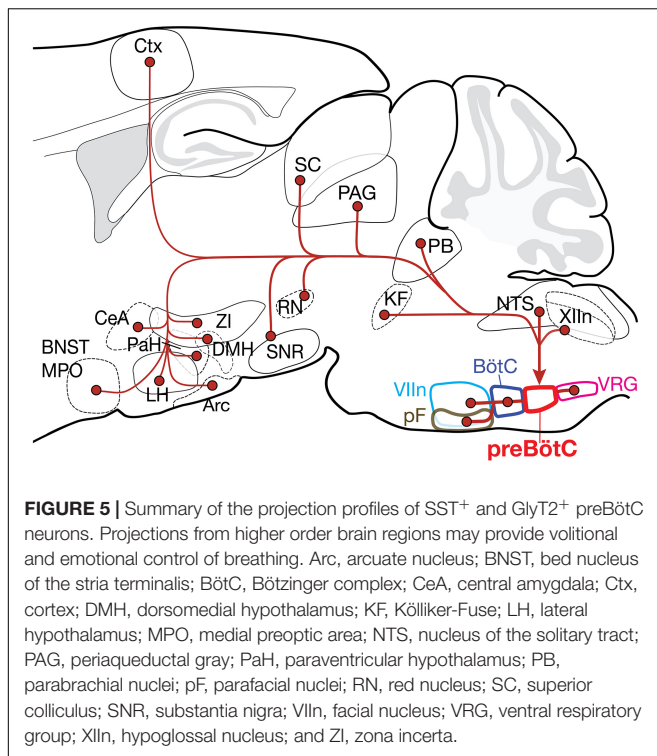
Strikingly, there were direct monosynaptic projections from the cortex and the amygdala. In cortex, mCherry$^+$ neurons were found in layer L5 or L5B (as L5A neurons are cortico-cortical) of motor cortex M1 (**Figures 4E,K**). These labeled cortical neurons were scattered along the rostral-caudal axis. We found neurons in what appeared to be layers 4 and 5 of sensory cortex S1, corresponding to the hindlimb and forelimb region. Within the amygdala, retrogradely labeled neurons were sparse but consistently localized to the central compartment (**Figures 4F,L**). For both the cortex and the amygdala, labeled neurons were present bilaterally, but more were found on the ipsilateral side of the injection. The mCherry-labeled cells were

more consistently found in the amygdala and cortex of SST-Cre mice than in GlyT2-Cre mice (cortex: 3 of 5 SST-Cre mice vs. 1 of 4 GlyT2-Cre mice; amygdala: 4 of 5 SST-Cre mice vs. 2 of 4 GlyT2-Cre mice). Although we did not always detect mCherry$^+$ neurons in every suprapontine region for each rabies-injected mouse, we did find mCherry$^+$ neurons in every suprapontine region for SST-Cre as well as GlyT2-Cre cohorts, indicating that afferent neurons in each of these site project onto both excitatory and inhibitory preBötC neurons.

DISCUSSION

As the kernel for the bCPG, the preBötC generates the inspiratory rhythm and transmits inspiratory-modulated signals to bulbospinal premotoneurons via projections to motoneurons innervating inspiratory muscles that underlie breathing movements. Thus, it is a ripe target for modulating breathing pattern. Here, we established multiple brainstem and suprapontine regions with monosynaptic projections to excitatory and inhibitory preBötC neurons (**Figure 5**). We first identified a panel of regions that project to the preBötC using a non-genetic tracer, allowing us to subsequently focus on regions most likely to contain retrogradely labeled cells using the modified rabies strategy. We consistently found Fluorogold-labeled neurons in regions reported to project to the preBötC

FIGURE 4 | Suprapontine afferent projections of SST$^+$ **(A–F)** and GlyT2$^+$ **(G–L)** preBötC neurons extend to the zona incerta, arcuate nucleus, lateral hypothalamus, and paraventricular hypothalamus, as well as the central amygdala (CeA) and motor/sensory cortex (M1/S1). Boxes in schematic represent location of images shown. Scale bar = 200 μm.

FIGURE 5 | Summary of the projection profiles of SST[+] and GlyT2^{+} preBötC neurons. Projections from higher order brain regions may provide volitional and emotional control of breathing. Arc, arcuate nucleus; BNST, bed nucleus of the stria terminalis; BötC, Bötzinger complex; CeA, central amygdala; Ctx, cortex; DMH, dorsomedial hypothalamus; KF, Kölliker-Fuse; LH, lateral hypothalamus; MPO, medial preoptic area; NTS, nucleus of the solitary tract; PAG, periaqueductal gray; PaH, paraventricular hypothalamus; PB, parabrachial nuclei; pF, parafacial nuclei; RN, red nucleus; SC, superior colliculus; SNR, substantia nigra; VIIn, facial nucleus; VRG, ventral respiratory group; XIIn, hypoglossal nucleus; and ZI, zona incerta.

but as with previous reports (Gang et al., 1995), it was impossible to limit the injection site to the preBötC or avoid transport by fibers of passage. Indeed, there were additional projections from regions that were not identified using the modified rabies strategy (see below), highlighting the specificity of our approach. Even so, given the low yield of retrograde labeling with modified rabies, we may be underestimating the strength of these projections or failing to detect sparse projections to the preBötC neurons. Nevertheless, despite a small population of preBötC starter cells, we show consistent retrograde labeling of presumptive targets that project to the preBötC. A survey of the functional connectivity and relative strengths of the brainstem and suprapontine connections to the bCPG will inform how higher-order brain regions signal through these projections to exert their influence on breathing.

Reciprocal preBötC Projections With Breathing-Related Regions in the Brainstem

Many brainstem regions reciprocally connect with the preBötC, representing recurrent circuits for feedback modulation of breathing. The bCPG includes a column of respiratory-related nuclei along the ventral medulla that interact with the preBötC (Alheid and McCrimmon, 2008). We now show that many of these regions project directly to both excitatory SST[+] and inhibitory GlyT2^{+} preBötC neurons. The BötC, just rostral to the preBötC, contains mostly inhibitory glycinergic neurons that are active during postinspiration and expiration (Ezure and Manabe, 1988; Ezure, 1990; Jiang and Lipski, 1990; Tian et al., 1999; Ezure et al., 2003) and receives projections from PB/KF nuclei, NTS,

and the parafacial region (Gang et al., 1995). Within the pF, we find more projections from the pF$_V$ to the preBötC than the pF$_L$. As the pF$_V$ provides chemosensory-related excitatory tone for breathing, it can do so via direct projections to preBötC SST[+] and GlyT2^{+} neurons, in addition to downstream projections to hypoglossal and phrenic (pre)motoneurons (Rosin et al., 2006; Chamberlin et al., 2007). There are projections originating dorsomedial to pF and BötC, the site of the presumptive PiCo (Anderson et al., 2016) to the preBötC; this projection could act to coordinate and sequence inspiration and post-inspiration.

The preBötC receives descending and ascending signals from other brainstem regions that can modulate its activity to affect breathing. The NTS receives sensory signals from vagus, facial, and glossopharyngeal nerves, as well as peripheral chemo-, baro-, and mechano-receptors; it also receives descending input from the forebrain originating from hypothalamus, including the paraventricular nucleus, amygdala (basolateral, central), and cortex (Schwaber et al., 1982; van der Kooy et al., 1984; Affleck et al., 2012) that can modulate the processing of these sensory signals. The NTS also contains premotoneurons critical for coordinating expiratory breaths for vocalizations (Hernandez-Miranda et al., 2017). From the pons, the preBötC receives direct input from PB/KF nuclei, which play a role in regulating the timing and phase transitions of the respiratory cycle. These regions are implicated in coupling vocalization, swallowing, and nociception to breathing (Dutschmann and Dick, 2012). The dorsolateral pons receives projections from the NTS, pF$_V$, amygdala, bed nucleus of the stria terminalis, hypothalamus, substantia nigra, and ventral tegmental area, thus providing the preBötC with integrated input from many modalities.

Suprapontine Projections to preBötC Relay Integrated Sensorimotor Information

Projections to the preBötC from the midbrain originate from structures that receive sensory information and process motor commands, therefore providing a means by which breathing could be modulated and coordinated with other behaviors. The periaqueductal gray (PAG) is postulated to integrate motor, limbic, and sensory information to modulate breathing across behaviors, such as gasping and vocalization, in a context-specific manner (Subramanian and Holstege, 2010). Stimulation of the PAG can change preBötC activity, and activation of different PAG divisions results in distinct breathing patterns. The superior colliculus transforms sensory information into motor output or behaviors, e.g., orienting, approach, or defensive behaviors (Gandhi and Katnani, 2011). Stimulation of the superior colliculus can change breathing (Keay et al., 1988). With direct projections to the preBötC from the superior colliculus, this pathway could coordinate breathing with specific behaviors, with minimal delay. While both the superior and inferior colliculi receive efferent projections from preBötC, retrogradely labeled neurons were almost exclusively in the superior colliculus. As the inferior colliculus primarily processes auditory signals, this suggests that other, perhaps indirect, pathways may coordinate

auditory-related behaviors with breathing or underlie audition-induced changes in breathing, as in the startle response (Fendt et al., 2001).

Both the substantia nigra and the red nucleus participate in motor coordination, but neither has been directly linked to neural pathways affecting breathing. An indirect pathway between the substantia nigra and the retrotrapezoid nucleus through the PAG is impacted in a Parkinson's model of respiratory failure in rats (Lima et al., 2018), and red nucleus neurons may play a role in regulating ventilatory response to hypoxia (Ackland et al., 1997). As the red nucleus and the substantia nigra are responsible for coordinating and facilitating movement, these regions could be relaying information to the preBötC to synchronize breathing with gait or other movements.

Descending afferent projections from the forebrain provide information regarding emotional, cognitive, and physiological state to the preBötC. With various hypothalamic nuclei projecting to the preBötC, there are potentially a broad range of regulatory behaviors that could directly and rapidly influence breathing. The arcuate nucleus regulates feeding behavior, energy homeostasis, and diurnal temperature, while the medial preoptic area is implicated in temperature regulation and sex-specific behaviors such as mating and aggression (Kumar, 2004; Sohn et al., 2013; Guzmán-Ruiz et al., 2015; Li and Dulac, 2018). The lateral and dorsomedial hypothalamus are involved in feeding, reward, sleep/wakefulness, and stress (Harris and Aston-Jones, 2006; Fontes et al., 2011; Arrigoni et al., 2018). These regions are rich in neurons that secrete peptides and hormones such as ghrelin, orexin, and melanin-concentrating hormone (MCH), which can affect the breathing across different arousal states (Benedetto et al., 2013). The hypothalamus is highly interconnected with the limbic and motor systems and could provide information to modulate breathing in relation to physiological or behavioral state.

Projections from the cortex to the preBötC were present throughout primary and secondary motor cortex. Although corticobulbar neurons from primary motor cortex innervate premotor and motoneurons in and around the trigeminal, facial, vagus, hypoglossal, and glossopharyngeal nucleus, no direct connections from the cortex to the preBötC had been identified. These projections could provide efference copy to the preBötC for behaviors that need to be timed with the breathing cycle, e.g., chewing, swallowing, and vocalization (Martin-Harris, 2006; Rea, 2015).

The CeA is the output pathway from amygdala to brainstem. While it contributes to the learning and expression of fear responses, e.g., fight or flight and emotional behavior, the CeA also modulates physiological responses to stress (Ressler, 2010; Fadok et al., 2018). Direct stimulation of the CeA across the breathing cycle results in a shift to inspiratory phase, and the activity of some CeA neurons are phase-locked with the breathing cycle (Harper et al., 1984; Frysinger et al., 1988). In humans, electrical stimulation of the amygdala results in an apnea (Dlouhy et al., 2015), suggesting that the amygdala is functionally coupled to the brainstem bCPG. The CeA receives input from cortex, limbic system, hypothalamus, olfactory pathway, substantia nigra, and many brainstem nuclei

(Usunoff et al., 2006; Bienkowski and Rinaman, 2013; Gu et al., 2020), and processes information to generate a breathing response to emotional stimuli, mediated at least in part by direct projections to the bCPG.

Functional Input to preBötC Neurons

Afferent inputs to the preBötC originate from different regions of the brain associated with different functions and contain neurons with diverse molecular phenotypes that will also likely corelease peptidergic and/or hormonal neuromodulators that influence breathing pattern, e.g., opioids, serotonin, orexin, SST, ghrelin, and MCH (Gray et al., 2001; Young et al., 2005; Mulkey et al., 2007). Depending on the phenotype of these neurons, the onset and duration of effects on breathing could span a broad range. Since afferent projections from each region project to both SST^+ and $GlyT2^+$ preBötC neurons, the net effect on preBötC activity will depend on whether the inputs from individual neurons are targeting one or both subpopulation(s), as well as their neurotransmitter/neuromodulator release and the associated postsynaptic receptors. Indeed, stimulation within the amygdala, even just the CeA, can result in a multitude of different breathing responses (Bonvallet and Gary-Bobo, 1971; Dlouhy et al., 2015).

Reciprocal Projections to the preBötC Allow Feedback Control

SST^+ and $GlyT2^+$ preBötC neurons project broadly within the brainstem and have select efferent suprapontine targets (Tan et al., 2010; Yang and Feldman, 2018). Many brainstem regions have reciprocal projections with the preBötC including pF, BötC, NTS, and PB/KF nuclei that could modulate and/or regulate the precise pattern of breathing. Surprisingly many suprapontine regions including superior colliculus, dorsomedial and lateral hypothalamus, and zona incerta also have reciprocal projections with excitatory and inhibitory preBötC neurons. Other regions projecting to preBötC, e.g., cortex, CeA, inferior colliculus, that do not appear to receive direct projections from SST^+ or $GlyT2^+$ preBötC neurons, could receive inputs from other preBötC cell types, e.g., SST^- glutamatergic or GABAergic neurons. Moreover, these regions could receive oligosynaptic input arising from preBötC. Respiratory activity can be detected in and phase-locked with oscillations in the cortex, hippocampus, and amygdala (Rojas-Libano et al., 2018), and such entrainment is postulated to contribute to cognitive functions including memory encoding and consolidation. In addition to ascending respiratory-related oscillations that appear to originate in olfactory sensory neurons (Moberly et al., 2018), direct or indirect pathways from bCPG are also capable of relaying respiratory rhythms to the forebrain (Yang and Feldman, 2018). Although we did not detect direct projections from hippocampus, prefrontal cortex, orbital cortex, or olfactory bulb to the brainstem, we did find such projections from motor cortex, central amygdala, and hypothalamic nuclei. Essential to note is that brain regions with sparse projections to the preBötC could be missed with our assay. Nonetheless, the direct afferent projections from the forebrain to the preBötC that we identified could represent a substrate for coordinating

inspiratory activity with other behaviors or physiology, e.g., cardiorespiratory coupling, vocalizations, whisking, feeding, sniffing, or cognitive processes (Kleinfeld et al., 2014).

Direct/Indirect Control of Breathing

The preBötC neuronal subpopulations targeted for retrograde tracing were either SST^+ or $GlyT2^+$ and account for only a portion of its excitatory and inhibitory population. Despite such a small target population, we identified a select list of brainstem and suprapontine regions that project directly onto preBötC neurons, indicating that the bCPG receives information across many modalities and suggesting considerable and complex modulation by emotional- and cognitive-related input. In addition to the input onto these preBötC populations, afferent information may also be introduced into the bCPG via targeting rhythmogenic preBötC neurons. Delineating the afferent input into the preBötC thus captures the flow of information in generating the inspiratory motor command and reveals potential pathways for higher-order control of breathing.

DATA AVAILABILITY STATEMENT

The datasets generated for this study are available on request to the corresponding author.

ETHICS STATEMENT

The animal study was reviewed and approved by the UCLA Institutional Animal Care and Use Committee.

AUTHOR CONTRIBUTIONS

CY and JF conceived and designed the study, contributed to the analysis, interpreted the results, and wrote the manuscript. CY carried out the experiments. EK and EC contributed with reagents for acquisition and analysis of the data. All authors contributed to manuscript revision, read, and approved the submitted version.

FUNDING

ACKNOWLEDGMENTS

SUPPLEMENTARY MATERIAL

The Supplementary Material for this article can be found online at: https://www.frontiersin.org/articles/10.3389/fnana.2020.00058/full#supplementary-material

FIGURE S1 | Retrograde labeling of putative afferent projections to the preBötC. Fluorogold injections into the preBötC [**(A)**, arrow] result in retrograde labeling of neurons throughout the brain including the nucleus of the solitary tract (NTS) contralateral preBötC, parafacial and facial (VIIn) nuclei, parabrachial nuclei and Kölliker-Fuse (PB/KF), trigeminal nucleus (MO5), substantia nigra, red nucleus, superior colliculus, central amygdala, lateral hypothalamus, and zona incerta, paraventricular hypothalamus, bed nucleus of the stria terminalis (BNST), lateral preoptic area (LPO), and cortex **(B–P)**. (ChAT staining, red), (scp, superior cerebellar peduncle) **(A)** Scale bar = 500 μm; **(B–P)** Scale bar = 200 μm.

REFERENCES

Ackland, G. L., Noble, R., and Hanson, M. A. (1997). Red nucleus inhibits breathing during hypoxia in neonates. *Respir. Physiol.* 110, 251–260. doi: 10.1016/s0034-5687(97)00090-x

Affleck, V. S., Coote, J. H., and Pyner, S. (2012). The projection and synaptic organisation of NTS afferent connections with presympathetic neurons, GABA and nNOS neurons in the paraventricular nucleus of the hypothalamus. *Neuroscience* 219, 48–61. doi: 10.1016/j.neuroscience.2012.05.070

Alheid, G. F., and McCrimmon, D. R. (2008). The chemical neuroanatomy of breathing. *Respir. Physiol. Neurobiol.* 164, 3–11. doi: 10.1016/j.resp.2008.07.014

Anderson, T. M., Garcia, A. J. III, Baertsch, N. A., Pollak, J., Bloom, J. C., Wei, A. D., et al. (2016). A novel excitatory network for the control of breathing. *Nature* 536, 76–80. doi: 10.1038/nature18944

Arrigoni, E., Chee, M. J. S., and Fuller, P. M. (2018). To eat or to sleep: That is a lateral hypothalamic question. *Neuropharmacology* 154, 34–49. doi: 10.1016/j.neuropharm.2018.11.017

Benedetto, L., Rodriguez-Servetti, Z., Lagos, P., D'Almeida, V., Monti, J. M., and Torterolo, P. (2013). Microinjection of melanin concentrating hormone into the lateral preoptic area promotes non-REM sleep in the rat. *Peptides* 39, 11–15. doi: 10.1016/j.peptides.2012.10.005

Bienkowski, M. S., and Rinaman, L. (2013). Common and distinct neural inputs to the medial central nucleus of the amygdala and anterior ventrolateral bed nucleus of stria terminalis in rats. *Brain Struct. Funct.* 218, 187–208. doi: 10.1007/s00429-012-0393-6

Boiten, F. A., Frijda, N. H., and Wientjes, C. J. (1994). Emotions and respiratory patterns: review and critical analysis. *Int. J. Psychophysiol.* 17, 103–128. doi: 10.1016/0167-8760(94)90027-2

Bonvallet, M., and Gary-Bobo, E. (1971). Effects of localized stimulations of the amygdaloid body on the amplitude of a monosynaptic reflex (masseter reflex). *J. Physiol.* 63:174A.

Callaway, E. M., and Luo, L. (2015). Monosynaptic circuit tracing with glycoprotein-deleted rabies viruses. *J. Neurosci.* 35, 8979–8985. doi: 10.1523/JNEUROSCI.0409-15.2015

Chamberlin, N. L., Eikermann, M., Fassbender, P., White, D. P., and Malhotra, A. (2007). Genioglossus premotoneurons and the negative pressure reflex in rats. *J. Physiol.* 579(Pt 2), 515–526. doi: 10.1113/jphysiol.2006.121889

Cui, Y., Kam, K., Sherman, D., Janczewski, W. A., Zheng, Y., and Feldman, J. L. (2016). Defining preBotzinger complex rhythm- and pattern-generating neural microcircuits in vivo. *Neuron* 91, 602–614. doi: 10.1016/j.neuron.2016.07.003

Del Negro, C. A., Funk, G. D., and Feldman, J. L. (2018). Breathing matters. *Nat. Rev. Neurosci.* 19, 351–367. doi: 10.1038/s41583-018-0003-6

Dlouhy, B. J., Gehlbach, B. K., Kreple, C. J., Kawasaki, H., Oya, H., Buzza, C., et al. (2015). Breathing inhibited when seizures spread to the amygdala and upon amygdala stimulation. *J. Neurosci.* 35, 10281–10289. doi: 10.1523/JNEUROSCI.0888-15.2015

Dutschmann, M., and Dick, T. E. (2012). Pontine mechanisms of respiratory control. *Compr. Physiol.* 2, 2443–2469. doi: 10.1002/cphy.c100015

Ezure, K. (1990). Synaptic connections between medullary respiratory neurons and considerations on the genesis of respiratory rhythm. *Prog. Neurobiol.* 35, 429–450. doi: 10.1016/0301-0082(90)90030-K

Ezure, K., and Manabe, M. (1988). Decrementing expiratory neurons of the Botzinger complex. II. Direct inhibitory synaptic linkage with ventral respiratory group neurons. *Exp. Brain Res.* 72, 159–166. doi: 10.1007/BF00248511

Ezure, K., Tanaka, I., and Kondo, M. (2003). Glycine is used as a transmitter by decrementing expiratory neurons of the ventrolateral medulla in the rat. *J. Neurosci.* 23, 8941–8948. doi: 10.1523/JNEUROSCI.23-26-08941.2003

Fadok, J. P., Markovic, M., Tovote, P., and Lüthi, A. (2018). New perspectives on central amygdala function. *Curr. Opin. Neurobiol.* 49, 141–147. doi: 10.1016/j.conb.2018.02.009

Feldman, J. L., Del Negro, C. A., and Gray, P. A. (2013). Understanding the rhythm of breathing: so near, yet so far. *Annu. Rev. Physiol.* 75, 423–452. doi: 10.1146/annurev-physiol-040510-130049

Fendt, M., Li, L., and Yeomans, J. S. (2001). Brain stem circuits mediating prepulse inhibition of the startle reflex. *Psychopharmacology* 156, 216–224. doi: 10.1007/s002130100794

Fontes, M. A., Xavier, C. H., de Menezes, R. C. A., and DiMicco, J. A. (2011). The dorsomedial hypothalamus and the central pathways involved in the cardiovascular response to emotional stress. *Neuroscience* 184, 64–74. doi: 10.1016/j.neuroscience.2011.03.018

Foster, E., Wildner, H., Tudeau, L., Haueter, S., Ralvenius, W. T., Jegen, M., et al. (2015). Targeted ablation, silencing, and activation establish glycinergic dorsal horn neurons as key components of a spinal gate for pain and itch. *Neuron* 85, 1289–1304. doi: 10.1016/j.neuron.2015.02.028

Frysinger, R. C., Zhang, J. X., and Harper, R. M. (1988). Cardiovascular and respiratory relationships with neuronal discharge in the central nucleus of the amygdala during sleep-waking states. *Sleep* 11, 317–332. doi: 10.1093/sleep/11.4.317

Gandhi, N. J., and Katnani, H. A. (2011). Motor functions of the superior colliculus. *Annu. Rev. Neurosci.* 34, 205–231. doi: 10.1146/annurev-neuro-061010-113728

Gang, S., Sato, Y., Kohama, I., and Aoki, M. (1995). Afferent projections to the Botzinger complex from the upper cervical cord and other respiratory related structures in the brainstem in cats: retrograde WGA-HRP tracing. *J. Auton. Nerv. Syst.* 56, 1–7. doi: 10.1016/0165-1838(95)00049-X

Gray, P. A., Janczewski, W. A., Mellen, N., McCrimmon, D. R., and Feldman, J. L. (2001). Normal breathing requires preBötzinger complex neurokinin-1 receptor-expressing neurons. *Nat. Neurosci.* 4, 927–930. doi: 10.1038/nn0901-927

Gu, Y., Piper, W. T., Branigan, L. A., Vazey, E. M., Aston-Jones, G., Lin, L., et al. (2020). A brainstem-central amygdala circuit underlies defensive responses to learned threats. *Mol. Psychiatry* 25, 640–654. doi: 10.1038/s41380-019-0599-6

Guzmán-Ruiz, M. A., Ramirez-Corona, A., Guerrero-Vargas, N. N., Sabath, E., Ramirez-Plascencia, O. D., Fuentes-Romero, R., et al. (2015). Role of the suprachiasmatic and arcuate nuclei in diurnal temperature regulation in the rat. *J. Neurosci.* 35, 15419–15429. doi: 10.1523/JNEUROSCI.1449-15.2015

Harper, R. M., Frysinger, R. C., Trelease, R. B., and Marks, J. D. (1984). State-dependent alteration of respiratory cycle timing by stimulation of the central nucleus of the amygdala. *Brain Res.* 306, 1–8. doi: 10.1016/0006-8993(84)90350-0

Harris, G. C., and Aston-Jones, G. (2006). Arousal and reward: a dichotomy in orexin function. *Trends Neurosci.* 29, 571–577. doi: 10.1016/j.tins.2006.08.002

Hernandez-Miranda, L. R., Ruffault, P. L., Bouvier, J. C., Murray, A. J., Morin-Surun, M. P., Zampieri, N., et al. (2017). Genetic identification of a hindbrain nucleus essential for innate vocalization. *Proc. Natl. Acad. Sci. U.S.A.* 114, 8095–8100. doi: 10.1073/pnas.1702893114

Huckstepp, R. T., Henderson, L. E., Cardoza, K. P., and Feldman, J. L. (2016). Interactions between respiratory oscillators in adult rats. *Elife* 5:e14203. doi: 10.7554/eLife.14203

Jiang, C., and Lipski, J. (1990). Extensive monosynaptic inhibition of ventral respiratory group neurons by augmenting neurons in the Botzinger complex in the cat. *Exp. Brain Res.* 81, 639–648. doi: 10.1007/BF02423514

Keay, K. A., Redgrave, P., and Dean, P. (1988). Cardiovascular and respiratory changes elicited by stimulation of rat superior colliculus. *Brain Res. Bull.* 20, 13–26. doi: 10.1016/j.resp.2015.10.012

Kim, E. J., Jacobs, M. W., Ito-Cole, T., and Callaway, E. M. (2016). Improved monosynaptic neural circuit tracing using engineered rabies virus glycoproteins. *Cell Rep.* 15, 692–699. doi: 10.1016/j.celrep.2016.03.067

Kim, E. J., Juavinett, A. L., Kyubwa, E. M., Jacobs, M. W., and Callaway, E. M. (2015). Three types of cortical layer 5 neurons that differ in brain-wide connectivity and function. *Neuron* 88, 1253–1267. doi: 10.1016/j.neuron.2015.11.002

Kleinfeld, D., Deschênes, M., Wang, F., and Moore, J. D. (2014). More than a rhythm of life: breathing as a binder of orofacial sensation. *Nat. Neurosci.* 17, 647–651. doi: 10.1038/nn.3693

Kumar, V. M. (2004). Body temperature and sleep: are they controlled by the same mechanism? *Sleep Biol. Rhythms* 2, 103–124. doi: 10.1111/j.1479-8425.2004.00136.x

Li, Y., and Dulac, C. (2018). Neural coding of sex-specific social information in the mouse brain. *Curr. Opin. Neurobiol.* 53, 120–130. doi: 10.1016/j.conb.2018.07.005

Lima, J. C., Oliveira, L. M., Botelho, M. T., Moreira, T. S., and Takakura, A. C. (2018). The involvement of the pathway connecting the substantia nigra, the periaqueductal gray matter and the retrotrapezoid nucleus in breathing control in a rat model of Parkinson's disease. *Exp. Neurol.* 302, 46–56. doi: 10.1016/j.expneurol.2018.01.003

Martin-Harris, B. (2006). Coordination of Respiration and Swallowing. *GI Motility Online.* doi: 10.1038/gimo10

Miyamichi, K., Shlomai-Fuchs, Y., Shu, M., Weissbourd, B. C., Luo, L., and Mizrahi, A. (2013). Dissecting local circuits: parvalbumin interneurons underlie broad feedback control of olfactory bulb output. *Neuron* 80, 1232–1245. doi: 10.1016/j.neuron.2013.08.027

Moberly, A. H., Schreck, M., Bhattarai, J. P., Zweifel, L. S., Luo, W., and Ma, M. (2018). Olfactory inputs modulate respiration-related rhythmic activity in the prefrontal cortex and freezing behavior. *Nat. Comm.* 9:1528. doi: 10.1038/s41467-018-03988-1

Morgado-Valle, C., Baca, S. M., and Feldman, J. L. (2010). Glycinergic pacemaker neurons in preBötzinger complex of neonatal mouse. *J. Neurosci.* 30, 3634–3639. doi: 10.1523/JNEUROSCI.3040-09.2010

Mulkey, D. K., Rosin, D. L., West, G., Takakura, A. C., Moreira, T. S., Bayliss, D. A., et al. (2007). Serotonergic neurons activate chemosensitive retrotrapezoid nucleus neurons by a pH-independent mechanism. *J. Neurosci.* 27, 14128–14138. doi: 10.1523/JNEUROSCI.4167-07.2007

Paxinos, G., and Franklin, K. B. J. (2004). *The Mouse Brain in Stereotaxic Coordinates* (Compact 2nd Edn). Amsterdam and Boston, MA: Elsevier Academic Press.

Rea, P. (2015). *Essential Clinical Anatomy of the Nervous System*, 1st Edn. Amsterdam: Academic Press.

Ressler, K. J. (2010). Amygdala activity, fear, and anxiety: modulation by stress. *Biol. Psychiatry* 15 67, 1117–1119. doi: 10.1016/j.biopsych.2010.04.027

Rojas-Libano, D., Wimmer Del Solar, J., Aguilar-Rivera, M., Montefusco-Siegmund, R., and Maldonado, P. E. (2018). Local cortical activity of distant brain areas can phase-lock to the olfactory bulb's respiratory rhythm in the freely behaving rat. *J. Neurophysiol.* 120, 960–972. doi: 10.1152/jn.00088.2018

Rosin, D. L., Chang, D. A., and Guyenet, P. G. (2006). Afferent and efferent connections of the rat retrotrapezoid nucleus. *J. Comp. Neurol.* 499, 64–89. doi: 10.1002/cne.21105

Schwaber, J. S., Kapp, B. S., Higgins, G. A., and Rapp, P. R. (1982). Amygdaloid and basal forebrain direct connections with the nucleus of the solitary tract and the dorsal motor nucleus. *J. Neurosci.* 2, 1424–1438. doi: 10.1523/JNEUROSCI.02-10-01424.1982

Sherman, D., Worrell, J. W., Cui, Y., and Feldman, J. L. (2015). Optogenetic perturbation of preBotzinger complex inhibitory neurons modulates respiratory pattern. *Nat Neurosci* 18, 408–414. doi: 10.1038/nn.3938

Sohn, J. W., Elmquist, J. K., and Williams, K. W. (2013). Neuronal circuits that regulate feeding behavior and metabolism. *Trends Neurosci.* 36, 504–512. doi: 10.1016/j.tins.2013.05.003

Stornetta, R. L., Rosin, D. L., Wang, H., Sevigny, C. P., Weston, M. C., and Guyenet, P. G. (2003). A group of glutamatergic interneurons expressing high levels

of both neurokinin-1 receptors and somatostatin identifies the region of the pre-Bötzinger complex. *J. Comp. Neurol.* 455, 499–512. doi: 10.1002/cne.10504

Subramanian, H. H., and Holstege, G. (2010). Periaqueductal gray control of breathing. *Adv. Exp. Med. Biol.* 669, 353–358. doi: 10.1007/978-1-4419-5692-7_72

Tan, W., Janczewski, W. A., Yang, P., Shao, X. M., Callaway, E. M., and Feldman, J. L. (2008). Silencing preBötzinger complex somatostatin-expressing neurons induces persistent apnea in awake rat. *Nat. Neurosci.* 11, 538–540. doi: 10.1038/nn.2104

Tan, W., Pagliardini, S., Yang, P., Janczewski, W. A., and Feldman, J. L. (2010). Projections of preBötzinger complex neurons in adult rats. *J. Comp. Neurol.* 518, 1862–1878. doi: 10.1002/cne.22308

Tian, G. F., Peever, J. H., and Duffin, J. (1999). Botzinger-complex, bulbospinal expiratory neurones monosynaptically inhibit ventral-group respiratory neurones in the decerebrate rat. *Exp. Brain Res.* 124, 173–180. doi: 10.1007/S002210050612

Usunoff, K. G., Itzev, D. E., Rolfs, A., Schmitt, O., and Wree, A. (2006). Brain stem afferent connections of the amygdala in the rat with special references to a projection from the parabigeminal nucleus: a fluorescent retrograde tracing study. *Anat. Embryol.* 211, 475–496. doi: 10.1007/s00429-006-0099-8

van der Kooy, D., Koda, L. Y., McGinty, J. F., Gerfen, C. R., and Bloom, F. E. (1984). The organization of projections from the cortex, amygdala, and hypothalamus to the nucleus of the solitary tract in rat. *J. Comp. Neurol.* 224, 1–24. doi: 10.1002/cne.902240102

Wall, N. R., Wickersham, I. R., Cetin, A., De La Parra, M., and Callaway, E. M. (2010). Monosynaptic circuit tracing in vivo through Cre-dependent targeting and complementation of modified rabies virus. *Proc. Natl. Acad. Sci. U.S.A.* 107, 21848–21853. doi: 10.1073/pnas.1011756107

Wickersham, I. R., Sullivan, H. A., and Seung, H. S. (2013). Axonal and subcellular labelling using modified rabies viral vectors. *Nat. Commun.* 4:2332. doi: 10.1038/ncomms3332

Yang, C. F., and Feldman, J. L. (2018). Efferent projections of excitatory and inhibitory preBotzinger complex neurons. *J. Comp. Neurol.* 526, 1389–1402. doi: 10.1002/cne.24415

Young, J. K., Wu, M., Manaye, K. F., Kc, P., Allard, J. S., Mack, S. O., et al. (2005). Orexin stimulates breathing via medullary and spinal pathways. *J. Appl. Physiol.* 98, 1387–1395. doi: 10.1152/japplphysiol.00914.2004